Mathematical Theory and Modeling
ISSN 2224-5804 (Paper) ISSN 2225-0522 (Online)
Vol.4, No.14, 2014

Numerical Simulation for the Transmission Dynamics of Avian Influenza

A R. Kimbir[1], T. Aboiyar[1] and P. N. Okolo[2*](corresponding author)
1 Department of Mathematics/Statistics/Computer Science, University of Agriculture, Makurdi, Nigeria
2 Department of Natural Sciences, Nasarawa State Polytechnic, Lafia, Nasarawa State, Nigeria
[*]Email of the corresponding author: patricknoahokolo@yahoo.com

Abstract

This paper presents numerical simulations for the transmission dynamics of avian influenza using the model formulated and analysed by Kimbir *etal* (2014). It is proved that the disease free equilibrium state is locally asymptotically stable whenever the reproduction number is less than unity. The implication is that if the reproduction number is less than unity, the infection is controlled or eradicated and the disease persists otherwise. The numerical simulations are consistent with the local stability of the disease-free states. The simulations further reveals that the infection transmission rate constitutes an essential parameter for an epidemic to occur, thus efforts should be geared at bringing the infection transmission to the lowest level in order to ensure eradication. It was also shown from the study that increasing culling of infected birds, will reduce the disease progression within the birds' population thereby, reducing the transmission of avian influenza. Effective isolation of infected individuals without culling is vital to eradicating the disease transmission, but a combined effective use of culling of infected birds and isolation of infected humans is a strong control measure against pandemics.

Key words: Avian influenza, Mathematical model, Basic reproduction number, Numerical simulations

1.0 INTRODUCTION

Avian influenza or bird- flu is a contagious disease of animals caused by influenza A virus that normally infects mostly birds and less commonly, pigs (Arora and Arora, 2008; Alexander, 2000). Infection with avian influenza A viruses in birds (wild and domestic) causes two main forms of diseases that are distinguished by low and high extremes of virulence, namely low pathogenic avian influenza (LPAI) and highly pathogenic avian influenza (HPAI). The 'low pathogenic' form may go undetected and usually causes only mild symptoms such as ruffled feathers and a drop in egg production in domestic poultry. However the high pathogenic form spreads more rapidly through flocks of poultry. The mortality can approach 100%, often within 48 hours (DeJong and Hien, 2006).

Most cases of avian influenza infection in humans have resulted from direct or close contact with infected poultry such as domesticated chickens, ducks and turkeys or surfaces contaminated with secretions and excretions from infected birds (De Jong and Hien, 2006).

A number of mathematical models both deterministic and stochastic have been used to predict the world wide spread of pandemic influenza and for comparing interventions aimed at preventing and controlling avian influenza. See for example, Ferguson *et al*, (2005); Derouich and Boutayeb (2008) and Srinivasa (2008). Okosun and Yusuf (2007); Srinivasa (2008); Derouich and Bontayeb (2008) presented various mathematical models for avian influenza (H5N1). These models do not explicitly take into account any control measures.
Kimbir *et al* (2014) formulated and analysed a model for the transmission dynamics of avian influenza the thrust of this study is to build on the model formulated and analysed by exploring numerical solutions to the model. The paper is organized as follows, in Section 2, we present a model by Kimbir *et al* (2014) consisting of ordinary differential equations (ODE) that describes the interaction between birds and human population and the underlying assumptions and establish the existence and local stability of the disease free equilibrium states. In Section 3, we explore the numerical results. Our conclusions are discussed in Section 4.

2.0 Model Formulation

In their work, Kimbir *et al* (2014) subdivide the total avian (birds) population at time *t*, denoted by $N_B(t)$ into susceptible wild birds, $S_W(t)$, susceptible domestic birds, $S_D(t)$, infected wild birds, $I_W(t)$, and infected domestic birds, $I_D(t)$, so that

$$N_B(t) = S_W(t) + S_D(t) + I_W(t) + I_D(t).$$

In the human population, they assume that humans infected with avian influenza cannot infect susceptible humans. Thus the total human population at time *t*, denoted by $N_H(t)$ is sub-divided into susceptible humans, $S_H(t)$, infected humans, $I_H(t)$, isolated infected humans, $Q_H(t)$, and recovered humans, $R_H(t)$, so that

$$N_H(t) = S_H(t) + I_H(t) + Q_H(t) + R_H(t)$$

The variables and parameters used in the model are defined in Table 1.

Table 1: Variables and Parameters used in the model and their description

Variable/Parameter	Description
$N_W(t)$	Total number of wild birds at time t
$N_D(t)$	Total number of domestic birds at time t
$N_H(t)$	Total number of humans at time t
$S_W(t)$	Total number of Susceptible wild birds at time t
$I_W(t)$	Total number of Infected wild birds at time t
$S_D(t)$	Total number of Susceptible domestic birds at time t
$I_D(t)$	Total number of Infected domestic birds at time t
$S_H(t)$	Total number of Susceptible humans at time t
$I_D(t)$	Total number of Infected humans at time t
$Q_H(t)$	Total number of Isolated humans with avian strain at time t
$R_H(t)$	Total number of Recovered humans at time t
β_W	Average birth rate in wild birds
β_D	Average birth rate in domestic birds
$\alpha_W, \alpha_D, \alpha_A$	Infection transmission rates for birds
η	Destruction (culling) rate for infected birds
δ_B	Natural death rate in birds
d_w	Flu induced death rate in wild birds
d_D	Flu induced death rate in domestic birds
β_H	Average birth rate in humans
δ_H	Natural death rate in humans
d_H	Flu induced death rate in humans
ε_H	Isolation rate for humans with avian stain
ϑ_H	Flu induced death rate in Isolated humans ($\vartheta_H < d_H$)
v	Recovery rate without immunity
γ	Recovery rate with substantial immunity
σ	Loose of immunity rate in recovered humans

A schematic flow diagram of the extended model for the birds' population and human population is shown in Figure 1 below.

Wild Birds

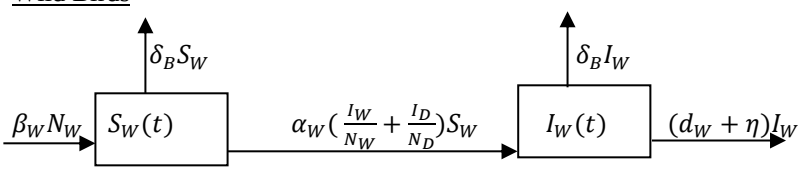

Domestic Birds

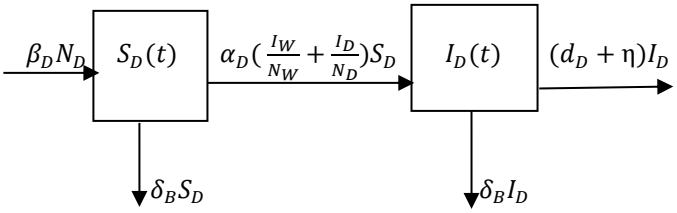

Humans

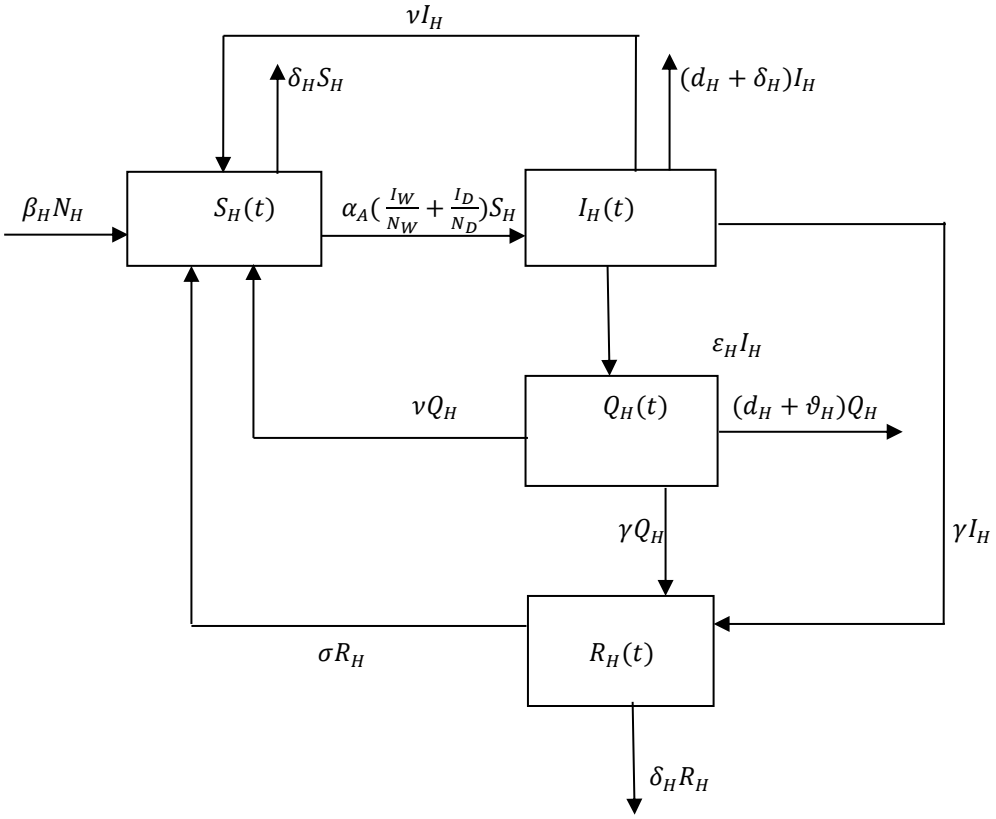

Figure 1: Schematic diagram of the transmission dynamics of avian influenza (H5N1) in birds and human population.

The above assumptions and schematic diagrams leads to the following system of ordinary differential equations

$$\frac{dS_W}{dt} = \beta_W N_W - \alpha_W\left(\frac{I_W}{N_W}+\frac{I_D}{N_D}\right)S_W - \delta_B S_W, \quad (1)$$

$$\frac{dI_W}{dt} = \alpha_W\left(\frac{I_W}{N_W}+\frac{I_D}{N_D}\right)S_W - (d_W+\delta_B+\eta)I_W, \quad (2)$$

$$\frac{dS_D}{dt} = \beta_D N_D - \alpha_D\left(\frac{I_W}{N_W}+\frac{I_D}{N_D}\right)S_D - \delta_B S_D, \quad (3)$$

$$\frac{dI_D}{dt} = \alpha_D\left(\frac{I_W}{N_W}+\frac{I_D}{N_D}\right)S_D - (d_D+\delta_D+\eta)I_D, \quad (4)$$

$$\frac{dS_H}{dt} = \beta_H N_H - \alpha_B \left(\frac{I_W}{N_W} + \frac{I_D}{N_D}\right) S_H - \delta_H S_H + \nu I_H + \nu Q_H + \sigma R_H, \quad (5)$$

$$\frac{dI_H}{dt} = \alpha_B \left(\frac{I_W}{N_W} + \frac{I_D}{N_D}\right) S_H - (\varepsilon_H + d_H + \delta_H + \nu + \gamma) I_H, \quad (6)$$

$$\frac{dQ_H}{dt} = \varepsilon_H I_H - (\nu + \vartheta_H + \gamma + \delta_H) Q_H, \quad (7)$$

$$\frac{dR_H}{dt} = \gamma I_H + \gamma Q_H - (\sigma + \delta_H) R_H, \quad (8)$$

For prevalence of the disease, it is necessary to consider the model in proportions of susceptible, infectious, isolated and recovered compartments.

Defining the proportion for each class as follows:

$$s_w = \frac{S_W}{N_W},\ i_W = \frac{I_W}{N_W}, s_D = \frac{S_D}{N_D},\ i_D = \frac{I_D}{N_D}, s_H = \frac{S_H}{N_H}, i_H = \frac{I_H}{N_H}, q_H = \frac{Q_H}{N_H}, r_H = \frac{R_H}{N_H},$$

so that

$$s_W + i_W = 1 \Rightarrow s_W = 1 - i_W, s_D + i_D = 1 \Rightarrow s_D = 1 - i_D$$

and

$$s_H + i_H + q_H + r_H = 1 \Rightarrow s_H = 1 - i_H - q_H - r_H$$

Thus, the system (1) – (8) expressed in proportion is given below:

$$\frac{ds_W}{dt} = \beta_W - \alpha_W(i_W + i_D)s_W - \beta_W s_W + (d_w + \eta) i_W s_W \quad (9)$$

$$\frac{di_W}{dt} = \alpha_W(i_W + i_D)s_w - (d_W + \beta_W + \eta) i_W + (d_w + \eta) i_W^2 \quad (10)$$

$$\frac{ds_D}{dt} = \beta_D - \alpha_D(i_W + i_D)s_D - \beta_D s_D + (d_D + \eta) i_D s_D \quad (11)$$

$$\frac{di_D}{dt} = \alpha_D(i_W + i_D)s_D - (d_D + \beta_D + \eta) i_D + (d_D + \eta) i_D^2 \quad (12)$$

$$\frac{ds_H}{dt} = \beta_H - \alpha_B(i_W + i_D)s_H + v(i_H + q_H) + \sigma r_H - \beta_H s_H + d_H s_H i_H + \vartheta_H s_H q_H \quad (13)$$

$$\frac{di_H}{dt} = \alpha_B(i_W + i_D)s_H - (\varepsilon + d_H + \beta_H + v + \gamma) i_H + \vartheta_H i_H q_H + d_H i_H^2 \quad (14)$$

$$\frac{dq_H}{dt} = \varepsilon_H i_H - (v + \vartheta_H + \gamma + \beta_H) q_H + d_H i_H q_H + \vartheta_H q_H^2 \quad (15)$$

$$\frac{dr_H}{dt} = \gamma i_H + \gamma q_H - (\sigma + \beta_H) r_H + d_H i_H r_H + \vartheta_H q_H r_H \quad (16)`$$

The system (9) – (16) can be reduced further by setting

$$s_W = 1 - i_W, s_D = 1 - i_D \text{ and } s_H = 1 - i_H - q_H - r_H$$

$$\frac{di_W}{dt} = \alpha_W(i_W + i_D)(1 - i_W) - (d_W + \beta_W + \eta) i_W + (d_w + \eta) i_W^2 \quad (17)$$

$$\frac{di_D}{dt} = \alpha_D(i_W + i_D)(1 - i_D) - (d_D + \beta_D + \eta) i_D + (d_D + \eta) i_D^2 \quad (18)$$

$$\frac{di_H}{dt} = \alpha_B(i_W + i_D)(1 - i_H - q_H - r_H) - (\varepsilon + d_H + \beta_H + v + \gamma) i_H + \vartheta_H i_H q_H + d_H i_H^2 \quad (19)$$

$$\frac{dq_H}{dt} = \varepsilon_H i_H - (v + \vartheta_H + \gamma + \beta_H)q_H + d_H i_H q_H + \vartheta_H q_H^2 \quad (20)$$

$$\frac{dr_H}{dt} = \gamma i_H + \gamma q_H - (\sigma + \beta_H)r_H + d_H i_H r_H + \vartheta_H q_H r_H \quad (21)`$$

These are the governing equations of the model.

2.1 Existence and Local Stability of the Disease-Free Equilibrium

The model in proportion given by equations (19) – (23) has a unique disease – free equilibrium state given by $\mathcal{E}_0 = (i_W, i_D, i_H, q_H, r_H) = (0,0,0,0,0)$ obtained by setting $i_W = 0, i_D = 0, i_H = 0, q_H = 0, r_H = 0$.

The local stability of $\mathcal{E}_0$ will be explored using the next generation operator method (Diekmann *et al.*, 1990; Van den Driessche and Watmough, 2002)., We rewrite the model equation which contribute to the transmission of infection, in this case the i_W, i_D and i_H classes. Thereafter write down matrix of infection rates F_i and the transition rate matrix V_i which represents rates of appearance of new infections into infective class and the transfer of individuals into and out of this class by all other means respectively.
The rate of appearance of new infection in compartments i_W, i_D and i_H are given by

$$F(x) = \begin{pmatrix} \alpha_W(i_W - i_W^2 + i_D - i_W i_D) \\ \alpha_D(i_W - i_W i_D + i_D - i_D^2) \\ \alpha_B(i_W + i_D)(1 - i_H - q_H - r_H) \end{pmatrix}.$$

While the remaining transfer terms in compartments i_W, i_D and i_H are given by

$$V(x) = \begin{pmatrix} (d_W + \beta_W + \eta)i_W - (d_w + \eta)i_W^2 \\ (d_D + \beta_D + \eta)i_D - (d_D + \eta)i_D^2 \\ (\varepsilon + d_H + \beta_H + v + \gamma)i_H - \vartheta_H i_H q_H + d_H i_H^2 \end{pmatrix}.$$

Taking partial derivatives of $F(x)$ with respect to i_W, i_D and i_H at the disease – free equilibrium state $\mathcal{E}_0 = (i_W, i_D, i_H, q_H, r_H) = (0,0,0,0,0)$, to obtain

$$F_x(\mathcal{E}_0) = \begin{pmatrix} \alpha_w & \alpha_w & 0 \\ \alpha_D & \alpha_D & 0 \\ \alpha_B & \alpha_B & 0 \end{pmatrix}.$$

Similarly the matrix of partial derivatives of $V(x)$ at the disease – free equilibrium state $\mathcal{E}_0 = (i_W, i_D, i_H, q_H, r_H) = (0,0,0,0,0)$ is given by

$$V_x(\mathcal{E}_0) = \begin{pmatrix} d_W + \beta_W + \eta & 0 & 0 \\ 0 & d_D + \beta_D + \eta & 0 \\ 0 & 0 & \varepsilon + d_H + \beta_H + v + \gamma \end{pmatrix}.$$

and

$$V_x^{-1}(\mathcal{E}_0) = \begin{pmatrix} \frac{1}{d_W + \beta_W + \eta} & 0 & 0 \\ 0 & \frac{1}{d_D + \beta_D + \eta} & 0 \\ 0 & 0 & \frac{1}{\varepsilon + d_H + \beta_H + v + \gamma} \end{pmatrix}.$$

Then

$$F_x(\mathcal{E}_0)V_x^{-1}(\mathcal{E}_0) = \begin{pmatrix} \frac{\alpha_w}{d_W+\beta_W+\eta} & \frac{\alpha_w}{d_D+\beta_D+\eta} & 0 \\ \frac{\alpha_D}{d_W+\beta_W+\eta} & \frac{\alpha_D}{d_D+\beta_D+\eta} & 0 \\ \frac{\alpha_B}{d_W+\beta_W+\eta} & \frac{\alpha_B}{d_D+\beta_D+\eta} & 0 \end{pmatrix}.$$

The eigenvalues are determined by solving the characteristic equation

$$\det(F_x(\mathcal{E}_0)V_x^{-1}(\mathcal{E}_0) - \lambda) = 0$$

$$det\begin{pmatrix} \frac{\alpha_w}{d_W+\beta_W+\eta} - \lambda & \frac{\alpha_w}{d_D+\beta_D+\eta} & 0 \\ \frac{\alpha_D}{d_W+\beta_W+\eta} & \frac{\alpha_D}{d_D+\beta_D+\eta} - \lambda & 0 \\ \frac{\alpha_B}{d_W+\beta_W+\eta} & \frac{\alpha_B}{d_D+\beta_D+\eta} & 0-\lambda \end{pmatrix} = 0$$

That is

$$(0-\lambda)\left[\left(\frac{\alpha_w}{d_W+\beta_W+\eta} - \lambda\right)\left(\frac{\alpha_D}{d_D+\beta_D+\eta} - \lambda\right) - \frac{\alpha_D}{d_W+\beta_W+\eta}\frac{\alpha_w}{d_D+\beta_D+\eta}\right] = 0$$

$$(0-\lambda)\left[\lambda^2 - \left(\frac{\alpha_w}{d_W+\beta_W+\eta} + \frac{\alpha_D}{d_D+\beta_D+\eta}\right)\lambda\right] = 0$$

$$(0-\lambda)\lambda\left[\lambda - \left(\frac{\alpha_w}{d_W+\beta_W+\eta} + \frac{\alpha_D}{d_D+\beta_D+\eta}\right)\right] = 0$$

$$\therefore\ \lambda = 0 \text{ or } \lambda = \frac{\alpha_w}{d_W+\beta_W+\eta} + \frac{\alpha_D}{d_D+\beta_D+\eta}$$

The maximum eigenvalue of $F_x(\mathcal{E}_0)V_x^{-1}(\mathcal{E}_0)$ is given as:

$$\lambda = \frac{\alpha_w}{d_W+\beta_W+\eta} + \frac{\alpha_D}{d_D+\beta_D+\eta}$$

Thus, the basic reproduction number is given as:

$$R_0 = \frac{\alpha_w}{d_W+\beta_W+\eta} + \frac{\alpha_D}{d_D+\beta_D+\eta} \qquad (30)$$

Thus we proved the following lemma.

Lemma 1: The DFEs of the model (19) – (23), given by $\mathcal{E}_0$, is locally asymptotically stable (LAS) if $R_0 < 1$ and $\mathcal{E}_0$ is unstable if $R_0 > 1$.

3.0 Numerical Simulations.

In order to carry out the numerical simulation, the parameters $\beta_W, \beta_D, \beta_H, \alpha_W, \alpha_D, \alpha_A, d_W, d_D, d_H, \delta_B, \delta_H, \eta, \varepsilon_H, \upsilon, \gamma,\ \sigma,\ \vartheta_H$ as defined section 3 are assigned specific values as well as the initial values of the variables i_W, i_D, i_H, q_H and r_H as shown in Table 1 below and subsequently implemented on MATLAB. It should be mentioned that all these parameters except η, ϑ_H and ε_H are estimated on the basis of some published data (Iwani *et al., 2009*; Chowell *et al., 2008*; Santrock, 2007; Wiraman, 2007; The Writing Committee of the World Health Organisation (WHO) Consultation on Human Influenza A/H5, 2006).

Table 2: TABLE SHOWING PARAMETER VALUES USED IN NUMERICAL SIMULATIONS

Parameter	Baseline value	Reference
$\beta_W, \beta_D, \beta_B$	0.6	Iwani *et al* (2009)
$\alpha_W, \alpha_D, \alpha_B$	0.3	Chowell *et al* (2008)
δ_B	1.37×10^{-3}	Iwani *et al* (2009)
d_W, d_D, d_B	0.1	Iwani *et al* (2009)
β_H	0.043	Iwani *et al* (2009)
d_H	0.1	The Writing Committee of the World Health Org. (WHO) Consultation on Human Influenza A/H5 (2006)
δ_H	4.2×10^{-5}	Santrock (2007)
v	1.7×10	Chowell *et al* (2008)
η	0.1	assumed
ε_H	0.3	assumed
ϑ_H	0.05	Chowell *et al* (2008)
γ	0.0017	Wiraman (2007)
σ	0.0009	Wiraman (2007)

TABLE 3: INITIAL VALUES FOR VARIABLES USED IN NUMERICAL SIMULATIONS.

Variable	Value	Reference
$s_W(0)$	0.98	Iwani *et al* (2009)
$i_W(0)$	0.02	Iwani *et al* (2009)
$s_D(0)$	0.98	Iwani *et al* (2009)
$i_D(0)$	0.02	Iwani *et al* (2009)
$s_H(0)$	0.99	assumed
$i_H(0)$	0.01	assumed
$q_H(0)$	0	assumed
$r_H(0)$	0	assumed

3.1 Numerical Experiments

3.1.1 Experiment 1

In this experiment we show how the disease progresses in the absence of intervention varying the infection transmission rates. Here, we wish to ascertain whether the solution profile will converge to the disease free equilibrium (DFE). The graph of the numerical results is presented in Figure 2.

3.1.2 Experiment 2.

The simulation was carried out similar to experiment 1 but with a "weak" control (culling of infected birds); we intend to illustrate the effect of culling of infected birds on the infected bird population using different infection transmission rates. The associated graph is shown in Figure 3.

3.1.3: Experiment 3.

This experiment has the same intention with Experiment 2, but with a "strong" culling (80% of the infected birds) rate. The numerical result and the associated graph is exhibited in Figure 4.

3.1.4: Experiment 4.

We consider the effect of culling of infected birds in the disease transmission in birds using three scenarios: one with "weak" control (culling) by setting the culling rate $\eta = 0.2$, the second with "average control (culling) by setting the culling rate $\eta = 0.5$, while the third has to do with "strong" control (culling) by setting the culling rate $\eta = 0.85$. The graph is displayed in Figure 5.

3.1.5 Experiment 5

Avian influenza transmission from birds to humans with no control strategy is the focus of this experiment. We wish to confirm whether the simulation with different infection transmission rate converges to the disease free equilibrium (DFE). The corresponding graph is presented in Figure 6.

3.1.6 Experiment 6.

In this experiment, single control measure was considered, that is the isolation of infected human without culling of infected birds. "Weak" isolation rate $\varepsilon_H = 0.1$ was used for the simulation. We wish to ascertain the effect of isolation of infected humans in avian influenza transmission and whether this simulation also converges to the disease free equilibrium. The graph is shown in Figure 7.

3.1.7: Experiment 7.

The simulation in this experiment is similar to Experiment 6 but with "strong" isolation rate, $\varepsilon_H = 0.6$ and different infection transmission rates. The graph is displayed in Figure 8.

3.1.8: Experiment 8

In this experiment, the simulation was based on three different isolation rates with no culling. We wish to ascertain the role or effect of isolation of infected humans in avian influenza eradication from human populations. The graph is shown in Figure 9.

3.1.9: Experiment 9.

This simulation is a combination of the two control strategies: culling of infected birds and isolation of infected humans. The experiment focused "weak" culling and the effect of isolation of infected humans in avian influenza transmission. The numerical result and the associated graph is exhibited in Figure 10.

3.1.10 Experiment 10

In this experiment, we focus on the effect of isolation of infected humans with "strong" culling for infected birds. We wish to ascertain the impact of these two control strategies in avian eradication in the human population. The graph is exhibited in Figure 11.

3.2 Numerical Results

The numerical results from Experiment 1 to Experiment 10 are tabulated in Table 3 – Table 12 (see Appendix A) and plotted graphically as presented in Figure 5 to Figure 14 below.

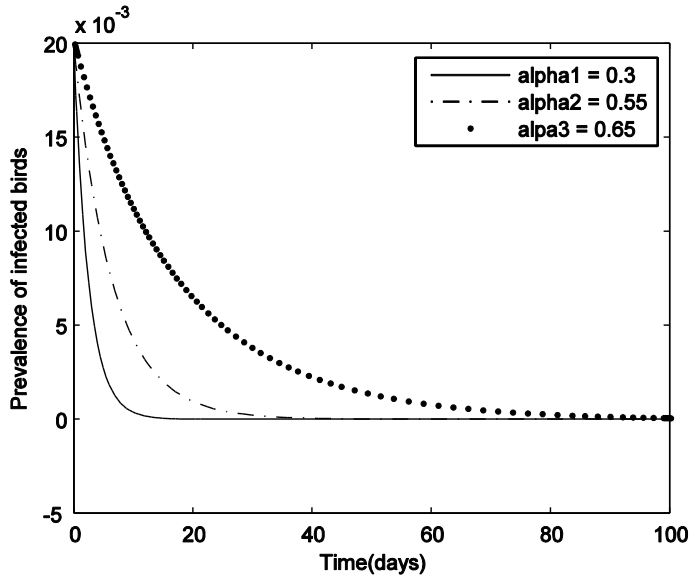

Figure 2: Prevalence of infected birds as a function of time with no control strategy ($R_0 < 1$), using different infection transmission rates, $\alpha_B = 0.3, 0.55$ and 0.65.

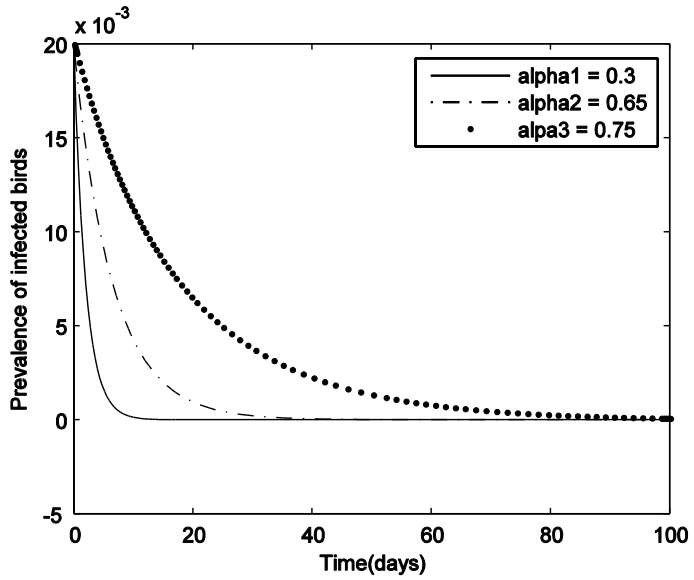

Figure 3: Prevalence of infected birds as a function of time with weak control (culling of infected birds) strategy using different infection transmission rates, $\alpha_B = 0.3, 0.65$ and 0.75.

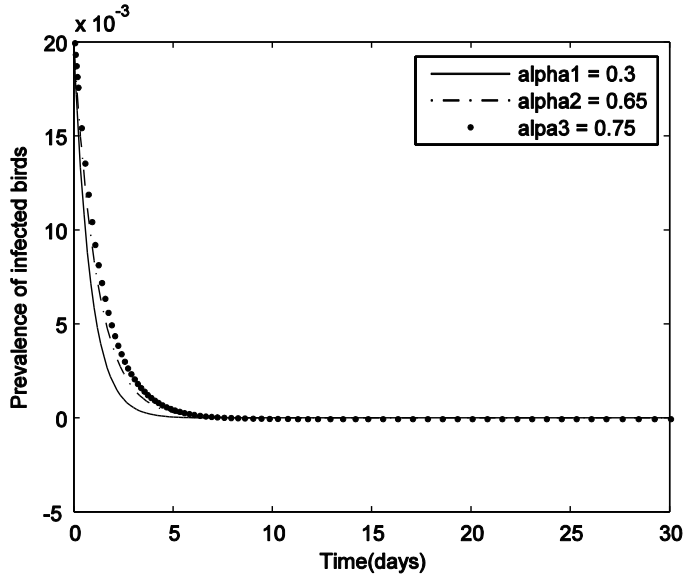

Figure 4: Prevalence of infected birds as a function of time with strong control (culling) strategy using different infection transmission rates, $\alpha_B = 0.3, 0.6$ and 0.75.

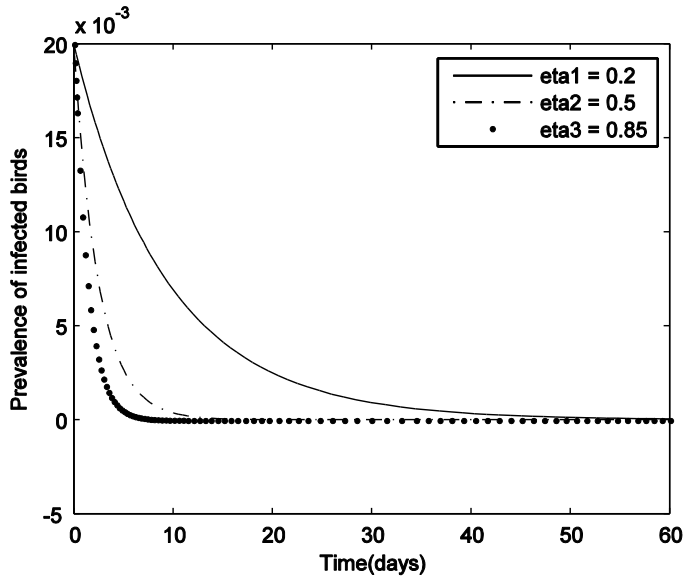

Figure 5: Effect of culling of infected birds on the proportion of infected birds as function of time.

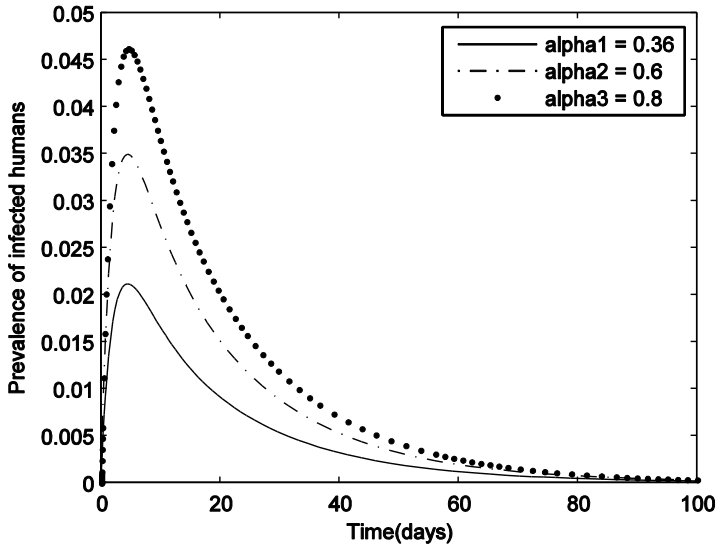

Figure 6: Prevalence of infected humans as a function of time with no control strategy ($R_0 < 1$), using different infection transmission rates, $\alpha_B = 0.36, 0.6$ and 0.8.

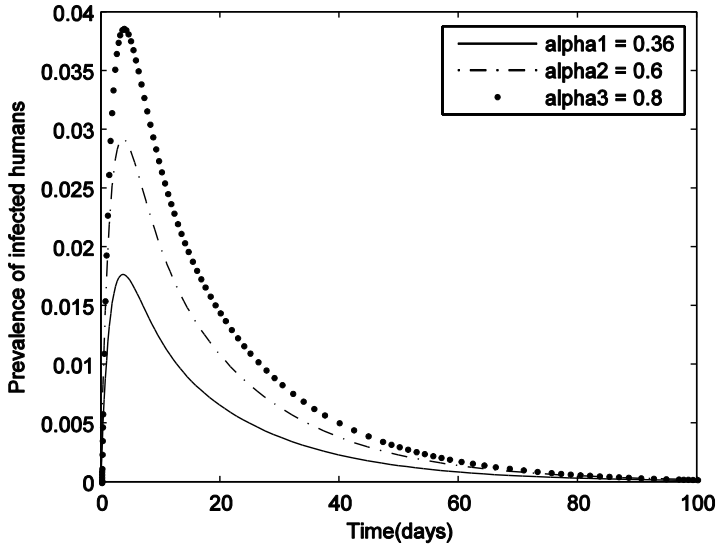

Figure 7: Prevalence of infected humans as a function of time with weak control (isolation) strategy using different infection transmission rates, $\alpha_B = 0.36, 0.6$ and 0.8.

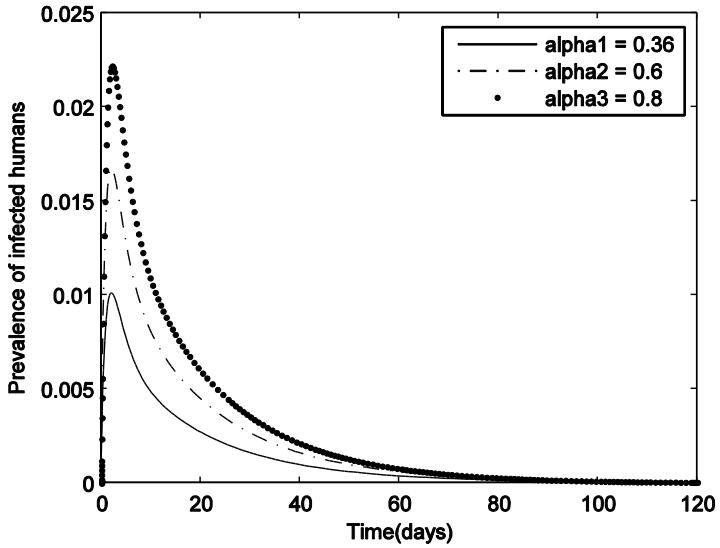

Figure 8: Prevalence of infected humans as a function of time with strong control strategy (isolation of infected human) using different infection transmission rates, $\alpha_B = 0.36, 0.6$ and 0.8.

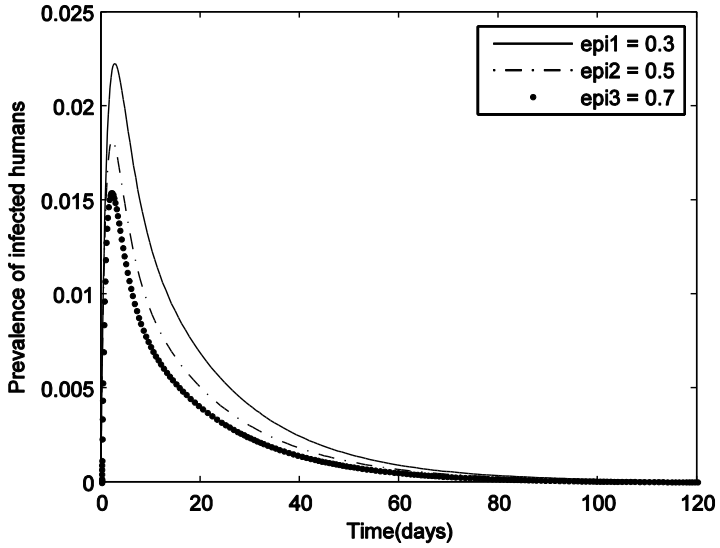

Figure. 9: Effect of isolation of infected human without culling of infected birds on the proportion of infected humans.

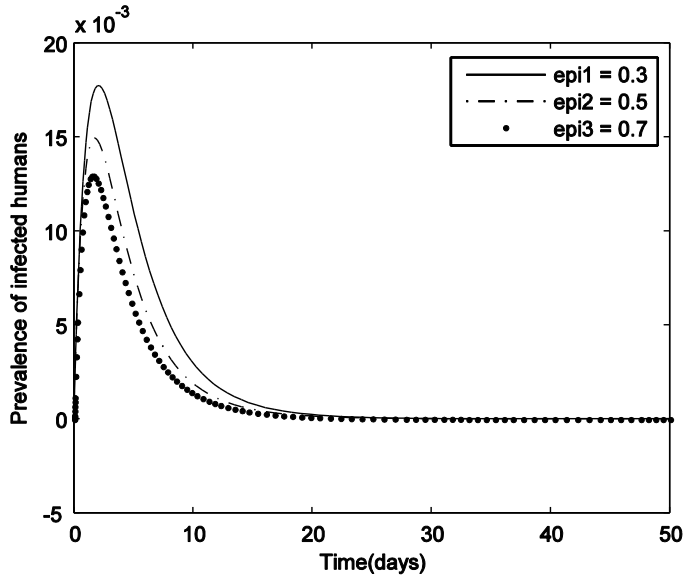

Figure 10: Effect of isolation of infected human with weak culling of infected birds on the proportion of infected humans.

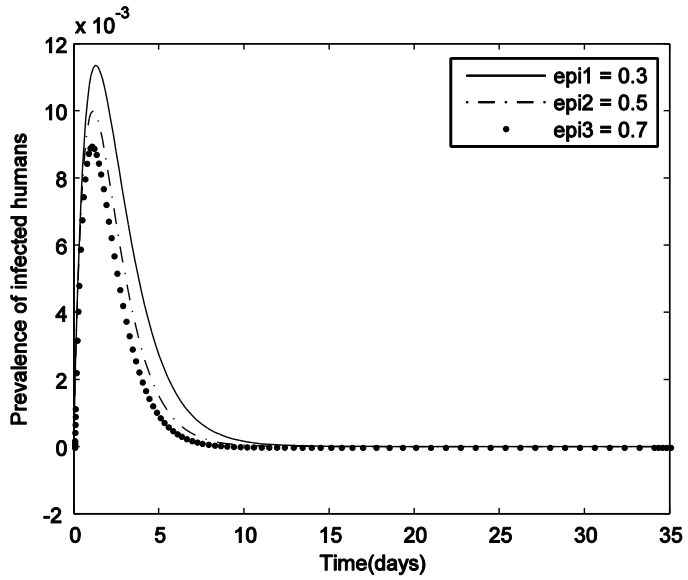

Figure 11: Effect of isolation of infected human with strong culling of infected birds on the proportion of infected humans.

3.3 Discussion

We will first discuss in this section how the disease progresses in the absence of intervention. Secondly when there is intervention in the form of culling of infected birds and lastly, the effects of isolation of infected humans. In each case we vary the most important parameters such as the infection transmission parameter, α, the culling rate for infected birds, η, and isolation rate for infected humans, ε.

Figure 2 shows increasing prevalence of avian influenza with increasing infection transmission rates ($\alpha_B = 0.3, 0.55, 0.65$)in the absence of any intervention ($\eta = 0$) . With the basic reproduction number, $R_0 < 1$ in each case, shows convergence of the solution profile to the disease free equilibrium (DFE). This is consistent with Lemma 1. The implication of this result is that, for an effective preventive strategy, effort should be geared at reducing the infection transmission rate.

Figure 3 shows increasing prevalence of avian influenza with increasing infection transmission rate ($\alpha_B = 0.3, 0.55, 0.65$)in the presence of weak culling rate ($\eta = 0.1$). There is no significant difference between Figure 2 and Figure 3 when the culling rate is weak ($\eta = 0.1$).

Figure 4 exhibit a decreasing prevalence of avian influenza in bird population when culling rate for infected birds is high ($\eta = 0.8$), even with increasing infection transmission rate ($\alpha_B = 0.3, 0.65, 0.75$). This Figure further reveals that with a strong culling ($\eta = 0.8$) of infected birds, the disease can be eradicated in the shortest possible time.

Similarly, Figure 5 shows decreasing prevalence of avian influenza with increasing culling rate ($\eta = 0.2, 0.5\ 0.85$). The stronger the culling rate, the shorter it takes for the eradication of the disease. The implication of this result is that effective culling of infected birds can be useful intervention for the control and eradication of avian influenza infection in avian population.

Figure 6 shows increasing prevalence of avian influenza infection in humans with increasing infection transmission rates ($\alpha_B = 0.3, 0.6, 0.8$) in the absence of any intervention ($\varepsilon = 0; \eta = 0$). Figure 6 shows convergence of the solution profile to the disease free equilibrium (DFE) with the basic reproduction number, $R_0 < 1$, which is consistent with Lemma 1. The implication is that, the infection transmission rate constitutes an essential key to preventive strategies against large outbreaks and that avian infection can be eradicated from the human population over time whenever $R_0 < 1$.

Figure 7 shows increasing prevalence of avian influenza infection in humans with increasing infection transmission rate ($\alpha_B = 0.36, 0.6, 0.8$) in the presence of weak isolation rate ($\varepsilon = 0.1$) and without culling of infected birds ($\eta = 0$).

Figure 8 exhibits a decreasing prevalence of avian influenza in human population when isolation rate of infected human is high ($\varepsilon = 0.6$) without culling of infected birds($\eta = 0$). Figure 8 further reveals that the higher (stronger) the isolation of infected humans the shorter it takes for the eradication of the disease.

Figure 9 shows decreasing prevalence of avian influenza with increasing isolation rate ($\varepsilon = 0.3, 0.5, 0.6$) without culling of infected birds ($\eta = 0$). Figure 9 further reveals that the higher the isolation rate, the shorter the time it will take to eradicate the disease.

Figure10 also shows a decreasing prevalence of avian influenza in humans with increasing isolation rates ($\varepsilon = 0.3, 0.5, 0.7$) and low culling rate($\eta = 0.2$). The Figure further shows that with a combination of high (strong) isolation of infected humans and low culling rate of infected birds the disease can be eradicated within a shorter period than only isolation of infected humans.

Figure11 shows decreasing prevalence of avian influenza with increasing isolation rate ($\varepsilon = 0.3, 0.5, 0.7$) and high culling rate ($\eta = 0.8$). This figure further reveals that with a combination of strong (high) culling of infected birds ($\eta = 0.8$) and high (strong) isolation of infected humans($\varepsilon = 0.7$), the disease can be eradicated in the shortest possible time. Thus a combination of isolation of infected individuals and the culling of infected birds as a control strategy is effective for the control and eradication of avian influenza.

4.0 Conclusion

We presented numerical simulations of a deterministic epidemiological model for the transmission dynamics of avian influenza. This study extended the model by Kimbir *et al* (2014) by exploring numerical solutions. It was established that the disease – free equilibrium state of model was locally asymptotically stable if $R_0 < 1$ and unstable if $R_0 > 1$.

Numerical solutions of the model were obtained using the fourth – order Runge – Kutta integration scheme coded in MATLAB. Numerical simulations of the model revealed that the infection transmission rate constitutes an essential key to preventive strategies against pandemics. Thus effort geared at reducing the infection transmission rate is a good and effective preventive strategy.

Numerical simulation further revealed that effective culling of infected birds or isolation of infected individual is a good control strategy for avian influenza infection. But combining effective culling of infected birds and isolation of infected individuals is crucial as a control measure against any pandemics.

REFERENCES

Alexander, D. J. (2000), A review of influenza in different bird species. *Vet Microbiol. 72 pp3 – 13*

Arora, D. R. and Arora, B. (2008), Text book of Microbiology(3rd Edition) CBS Publishers & Distributors, New Delhi.

Chowell, G., Miller, M. A. and Viboud, C. (2008). Seasonal influenza in the United States, France and Australia: transmission and progress for control. *Epidemiol. Infect. 136, 852 – 864.*

De Jong, M. D. and Hein, T. T. (2006), Avian influenza A (H5N1), *Journal of Clinical Virol., 35 pp 2 – 13*

Derouich, M. and Boutyeb, A. (2008), An avian influenza mathematical model. *Applied Mathematical Sciences, 2 (36) pp 1749 - 1760*

Diekmann, J. A., Heesterbeek, P. and Metz, J. A. J. (1990), On the definition and computation of basic reproduction ratio R_o in models of infectious diseases in heterogeneous populations. *Journal of Mathematical Biology, Sringer – verlag, 28 pp 365 – 382.*

Ferguson, N. M., Cummings, D. A. T., Fraser, C., Riley, S., Meeyai, A.,Iamsirithaworn, S. & Burke, D. S.(2005), Strategies for containing an emerging influenza pandemic in South east Asia. *Nature, 437 pp 209 – 214.*

Iwani, S., Takeuchi, Y. and Liu, X. (2009). Avian flu pandemic: Can we prevent it? *Journal of Theoretical Biology, 257, 181 – 190.*

Kimbir, A. R., Aboiyar, T. and Okolo, P. N. (2014). A Model Analysis for the Transmission Dynamics of Avian Influenza. *Journal of Mathematical Theory and Modeling , 4(13) pp 15 - 28*

Okosun, K. O., and Yusuf, T. T. (2007), Numerical Simulation of Bird flu Epidemics. *Research Journal of Applied Sciences 2(1) pp 9 – 12*

Santrock, J. (2007). Life expectancy. A Tropical Approach to: Life – span Development . New York, New York: The McGraw – Hill Companies, Inc.

Srinivasa, A. S. R. (2008), Modeling the rapid spread of avian influenza (H5N1) in India. *Mathematical Biosciences and Engineering, 5(3) pp 523 – 537*

The Writing Committee of the World Health Organisation (WHO) Consultation on Human influenza A/H5, (2006). Avian influenza H5N1, Thailand, 2004. *Emerging Infectious Diseases, 11 pp 1664 – 1672 [Pub Med]*

Van den Driessche, P., and Watmough, J. (2002). Reproduction numbers and sub-threshold endemic equilibra for compartmental models of disease transmission. *Mathematical Biosciences, 180, 28 – 48.*

Wiraman, C. (2007). Numerical Modelling of the transmission Dynamics of Influenza. The 1st Symposium on Optimization and System Biology, Beijing, China, 8th – 10th August, 2007.

The IISTE is a pioneer in the Open-Access hosting service and academic event management. The aim of the firm is Accelerating Global Knowledge Sharing.

More information about the firm can be found on the homepage:
http://www.iiste.org

CALL FOR JOURNAL PAPERS

There are more than 30 peer-reviewed academic journals hosted under the hosting platform.

Prospective authors of journals can find the submission instruction on the following page: http://www.iiste.org/journals/ All the journals articles are available online to the readers all over the world without financial, legal, or technical barriers other than those inseparable from gaining access to the internet itself. Paper version of the journals is also available upon request of readers and authors.

MORE RESOURCES

Book publication information: http://www.iiste.org/book/

Academic conference: http://www.iiste.org/conference/upcoming-conferences-call-for-paper/

IISTE Knowledge Sharing Partners

EBSCO, Index Copernicus, Ulrich's Periodicals Directory, JournalTOCS, PKP Open Archives Harvester, Bielefeld Academic Search Engine, Elektronische Zeitschriftenbibliothek EZB, Open J-Gate, OCLC WorldCat, Universe Digtial Library , NewJour, Google Scholar